

# Oscillator strengths and radiative transition rates for K<sub>α</sub> lines in gold X-ray spectra: 1s–2p transitions

Sultana N. Nahar\*, Anil K. Pradhan, Chiranjib Sur

*Department of Astronomy, The Ohio State University, Columbus, OH 43210, USA*

Received 19 July 2007; received in revised form 9 January 2008; accepted 12 January 2008

---

## Abstract

Oscillator strengths ( $f$ ), line strengths ( $S$ ) and radiative decay rates ( $A$ ) are presented for all 1s–2p transitions in gold (Au) ions. X-ray emission from gold is extensively used, such as in fusion experiments, and in medical research for diagnostics and treatment. The K<sub>α</sub> 1s–2p transitions in gold are found to be in the hard X-ray region of 66–73 keV (0.1888–0.1706 Å) and are limited to from hydrogen-like to fluorine-like ions as the 2p subshell is filled beyond fluorine. While there are two 1s–2p transitions ( $1s^2S_{1/2}-2p^2P_{1/2}^o$  and  $1s^2S_{1/2}-2p^2P_{3/2}^o$ ) for hydrogen-like gold, Au<sup>+78</sup>, the number varies depending on the number of electrons in the 2p subshell before and after the transition. For example, there are 35 1s–2p transitions giving the same number of K<sub>α</sub> lines for carbon-like Au, Au<sup>+73</sup>. The transitions can be of both types, dipole allowed and intercombination, and are in general strong, that is,  $A \sim 10^{16}/s$ . However, there are also weak transitions in the set. The present results are obtained from configuration interaction atomic structure calculations using the code SUPERSTRUCTURE which includes relativistic effects in Breit–Pauli approximation. The results have been benchmarked for a few ionic states with other detailed relativistic approaches, such as Dirac–Fock and coupled cluster. Comparisons with the very few transitions in the literature as well as those from other approaches indicate reasonable accuracy for the present results.

© 2008 Elsevier Ltd. All rights reserved.

PACS: 31.10.+z; 31.25.Jf; 32.30.-r; 32.30.Rj; 32.70.Cs; 36.20.Kd

Keywords: 1s–2p transitions; X-ray spectra; H- to F-like gold ions

---

## 1. Introduction

Gold is commonly used in many applications as an X-ray source. One of its most useful property is that it does not readily oxidize, or otherwise react chemically. In inertial confinement fusion experiments a thin layer of gold is included in the film which produces highly energetic X-ray photons. Gold X-rays from transition/ionization may be used to study the nuclear excitations [1]. Normally, atomic and nuclear energies are separated by keV to MeV. But for heavy atoms, the innermost (K-shell) electrons can have binding energies comparable to some nuclear transition energies, making it possible to excite the nucleus. In the opposite

---

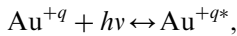
\*Corresponding author. Tel.: +1 614 292 1888; fax: +1 614 292 2928.

E-mail address: [nahar@astronomy.ohio-state.edu](mailto:nahar@astronomy.ohio-state.edu) (S.N. Nahar).

process a  $K_{\alpha}$  emission is possible from de-excitation of the nucleus. Recently gold has also been an important element in biomedical research because its X-ray absorption far exceeds that of body tissue, and it is non-toxic. It is found that X-rays absorbed by gold nanoparticles are capable of enhancing the efficiency of radiotherapy [2]. Gold nanoparticles attached to cancer cells and irradiated with 120–250 keV X-rays are found to kill cancerous cells more effectively [3].

Krypton K-shell X-ray spectra was recorded by the high energy electronic X-ray (HENEX) spectrometer from Li- to N-like Kr [4]. They provide new features in diagnostics on temperature, density, plasma opacity, and charge distribution. The authors expect to be able to carry out experiments for gold and other high-Z elements with energies beyond 60 keV.  $K_{\alpha}$  emission from gold targets were detected in National Ignition Facility (NIF) in filtered diodes (quoted in [4]). In a review article on high energy density physics, Hudson et al. [5] refer to achieving controlled thermonuclear ignition for alternative energy sources and discuss extending existing diagnostic techniques to high-Z, K-shell spectroscopy, such as for gold.

However, compared to extensive experimental observations and usage, there are very few theoretical studies for the radiative transition rates for various ionic states of gold (Au) of charge  $q$ ,



especially from the K-shell. The few available investigations are limited to H-, He-, and Li-like gold. This paper presents the oscillator strengths ( $f$ ), line strengths ( $S$ ), and radiative decay rates ( $A$ ) for  $K_{\alpha}$  radiation due to 1s–2p transitions for nine ionic states of gold. The results are obtained from configuration interaction atomic structure calculations using the code SUPERSTRUCTURE (SS) [6,7]. The relativistic effects are included through the Breit–Pauli (BP) approximation. The present relativistic results should be of sufficient accuracy until more detailed fully relativistic results are available.

## 2. Theory

Theoretical details of the present configuration interaction relativistic atomic structure calculations using SS can be found in [6–9]. A brief outline of the theory is given below.

In atomic structure calculations, the energies and wavefunctions of an  $N$ -electron ion are obtained through optimum solutions of the Schrodinger equation,

$$H_{\text{NR}} \Psi = \left[ \sum_{i=1}^N \left\{ -\nabla_i^2 - \frac{2Z}{r_i} + \sum_{j>i}^N \frac{2}{r_{ij}} \right\} \right] \Psi = E \Psi, \quad (1)$$

where  $\Psi = \Psi(\gamma SLM_S M_L | \mathbf{r}_1, \dots, \mathbf{r}_N)$  are the bound solutions consisting of a linear combination of configuration state functions.  $H_{\text{NR}}$  is the non-relativistic Hamiltonian. The antisymmetrization of the wavefunction is carried out by an expansion of products of single particle wavefunctions. The present approximation represents the nuclear and electron-electron potential by the statistical Thomas–Fermi–Dirac–Amaldi model potential

$$V^{\text{SM}}(r) = \frac{Z_{\text{eff}}(\lambda_{\text{nl}}, r)}{r}, \quad (2)$$

where  $Z_{\text{eff}}(\lambda_{\text{nl}}, r) = Z[e^{-Zr/2} + \lambda_{\text{nl}}(1 - e^{-Zr/2})]$ .  $\lambda_{\text{nl}}$  are the Thomas–Fermi scaling parameters for the orbitals.

The relativistic  $N$ -electron Hamiltonian in the BP approximation is written as (e.g. [9,10])

$$H_{\text{BP}} = H_{\text{NR}} + H_{\text{mass}} + H_{\text{Dar}} + H_{so} + \frac{1}{2} \sum_{i \neq j}^N [g_{ij}(so + so') + g_{ij}(ss') + g_{ij}(css') + g_{ij}(d) + g_{ij}(oo')], \quad (3)$$

where  $H_{\text{NR}}$  is the non-relativistic Hamiltonian, and

$$H_{\text{mass}} = -\frac{\alpha^2}{4} \sum_i p_i^4, \quad H_{\text{Dar}} = -\frac{\alpha^2}{4} \sum_i \nabla^2 \left( \frac{Z}{r_i} \right), \quad H_{so} = \alpha^2 \sum_{i=1}^N \frac{Z}{r_i^3} l(i) \cdot s(i) \quad (4)$$

are the relativistic one-body mass correction, Darwin, and spin–orbit interaction terms. The rest are two-body interaction terms with notation  $c$  for contraction,  $d$  for Darwin,  $o$  for orbit,  $s$  for spin and an apostrophe

indicates ‘other’. The present relativistic calculation includes the three one-body corrections terms and the first two two-body terms of full Breit interaction. Breit interaction ( $H^B$ ) consists of fine structure terms, that is, spin-other-orbit (so') and spin-other-spin (ss') terms:

$$H^B = \sum_{i>j} [g_{ij}(so + so') + g_{ij}(ss')], \quad (5)$$

where

$$\begin{aligned} g_{ij}(so + so') &= -\alpha^2 \left( \frac{\mathbf{r}_{ij}}{r_{ij}^3} \times \mathbf{p}_i \right) \cdot (\mathbf{s}_i + 2\mathbf{s}_j) + \left( \frac{\mathbf{r}_{ij}}{r_{ij}^3} \times \mathbf{p}_j \right) \cdot (\mathbf{s}_j + 2\mathbf{s}_i), \\ g_{ij}(ss') &= 2\alpha^2 \frac{\mathbf{s}_i \cdot \mathbf{s}_j}{r_{ij}^3} - 3 \frac{(\mathbf{s}_i \cdot \mathbf{r}_{ij})(\mathbf{s}_j \cdot \mathbf{r}_{ij})}{r_{ij}^5}, \end{aligned} \quad (6)$$

where  $\mathbf{p}$  is the momentum,  $\mathbf{s}$  is the spin, and  $\alpha$  is the fine structure constant.

Electric dipole-allowed E1 transitions ( $\Delta J = 0, \pm 1$ , parity ( $\pi$ ) changes, that is, odd parity  $\rightleftharpoons$  even parity) include both allowed same-spin-multiplets ( $\Delta L = 0, \pm 1, \pm 2$ ,  $\Delta S = 0$ ) and intercombination ( $\Delta L = 0, \pm 1 \pm 2$ ,  $\Delta S \neq 0$ ) transitions. (Note that the monopole  $\Delta J = 0-0$  transition is not allowed.) The line strength for electric dipole  $i-j$  transition is defined as

$$S(ij) = \left| \left\langle \Psi_j \left| \sum_{p=1}^N r_p \right| \Psi_i \right\rangle \right|^2, \quad S(ji) = S(ij), \quad (7)$$

where  $N$  is the number of electrons in the ion.  $S(ij)$  does not explicitly depend on the transition energy. Einstein's  $A$ -coefficient or the radiative decay rates and absorption oscillator strengths ( $f$ -values) for transitions between levels  $i$  and  $j$  for E1 transitions are obtained as

$$f_{ij} = \frac{E_{ji}}{3g_i} S(ij), \quad g_i f_{ij} = -g_j f_{ji}, \quad A_{ji} \cdot \tau_0 = \alpha^3 \frac{g_i}{g_j} E_{ji}^2 f_{ij}, \quad (8)$$

where the energy is in units of Ry =  $(\alpha^2/2)m_{\text{el}}c^2 = 13.6 \text{ eV}$ , and the time unit is  $\tau_0 = \hbar/\text{Ry} = 4.838 \times 10^{-17} \text{ s}$ ;  $E_{ij} = E_j - E_i$  is the excitation energy,  $g_j$  and  $g_i$  are the statistical weights of the upper and lower states, respectively.

The lifetime of a level can be computed as

$$\tau_k = \frac{1}{\sum_i A_{ki}}, \quad (9)$$

where the sum is the total radiative transition probability for level  $k$ .

### 3. Results and discussions

Oscillator strengths ( $f$ ), line strengths ( $S$ ) and radiative decay rates for the 1s–2p transition array producing  $K_\alpha$  lines are reported for nine ionic states of gold, from H-like  $\text{Au}^{+78}$  to F-like  $\text{Au}^{+70}$ . There are no bound–bound 1s–2p transition beyond fluorine because of the filled 2p subshell, although resonant fluorescent emission or photo-excitation is possible in any ion or neutral atom if a vacancy exists in the K-shell or the L-shell, respectively.

Each ionic state of gold has been represented by a relatively large set of configurations as listed in Table 1. For configuration interaction calculations it is important for higher accuracy to include all configurations that contribute most to the transitional symmetries. For example, for the  ${}^1\text{S}_0$  symmetry of He-like  $\text{Au}^{+77}$ , in addition to the ground configuration  $1s^2$  that forms  ${}^1\text{S}_0$ , other configurations, such as  $1s2s, 1s3s, 1s4s, 2p3p, 2p4p, 2s^2, 2p^2, 3s^2, 3p^2, 4s^2, 4p^2$ , etc. (Table 1) which also form  ${}^1\text{S}_0$  level, should be included for contributions to the symmetry. Although the list of configurations in Table 1 are expected to give accurate results, in absence of observed energies and accurate calculations, proper optimization for most of the ions cannot be verified by comparison. A low- $Z$  ion isoelectronic with a given gold ion was optimized first, and the

Table 1

List of configurations used for the atomic structure calculations for energies and oscillator strengths of various ionic states of Au

Au<sup>+78</sup>

1s(1), 2s(2), 2p(3), 3s(4), 3p(5), 3d(6), 4s(7), 4p(8), 4d(9), 4f(10)

Au<sup>+77</sup>

1s<sup>2</sup>(1), 1s2s(2), 1s2p(3), 1s3s(4), 1s3p(5), 1s3d(6), 1s4s(7), 1s4p(8), 1s4d(9), 1s4f(10), 2s<sup>2</sup>(11),  
 2p<sup>2</sup>(12), 3s<sup>2</sup>(13), 3p<sup>2</sup>(14), 3d<sup>2</sup>(15), 3d<sup>2</sup>(16), 2s2p(17), 2s3s(18), 2s3p(19), 2s3d(20), 2s4s(21),  
 2s4p(22), 2s4d(23), 2s4f(24), 2p3s(25), 2p3p(26), 2p3d(27), 2p4s(28), 2p4p(29)

Au<sup>+76</sup>

1s<sup>2</sup>2s(1), 1s<sup>2</sup>2p(2), 1s<sup>2</sup>3s(3), 1s<sup>2</sup>3p(4), 1s<sup>2</sup>3d(5), 1s<sup>2</sup>4s(6), 1s<sup>2</sup>4p(7), 1s<sup>2</sup>4d(8), 1s<sup>2</sup>4f(9), 1s2s<sup>2</sup>(10),  
 1s2s2p(11), 1s2s3s(12), 1s2s3p(13), 1s2s3d(14), 1s2s4s(15), 1s2s4p(16), 1s2s4d(17), 1s2s4f(18),  
 1s2p3s(19), 1s2p3p(20), 1s2p3d(21), 1s2p4s(22), 1s2p4p(23), 1s2p<sup>2</sup>(24), 1s3s<sup>2</sup>(25), 1s3p<sup>2</sup>(26),  
 1s3d<sup>2</sup>(27)

Au<sup>+75</sup>

1s<sup>2</sup>2s<sup>2</sup>(1), 1s<sup>2</sup>2s2p(2), 1s<sup>2</sup>2p<sup>2</sup>(3), 1s<sup>2</sup>2s3s(4), 1s<sup>2</sup>2s3p(5), 1s<sup>2</sup>2s3d(6), 1s<sup>2</sup>2s4s(7), 1s<sup>2</sup>2s4p(8),  
 1s<sup>2</sup>2s4d(9), 1s<sup>2</sup>2s4f(10), 1s<sup>2</sup>2p3s(11), 1s<sup>2</sup>2p3p(12), 1s<sup>2</sup>2p3d(13), 1s<sup>2</sup>2p4s(14), 1s<sup>2</sup>2p4p(15),  
 1s<sup>2</sup>2p4d(16), 1s<sup>2</sup>2p4f(17), 1s<sup>2</sup>2s5s(18), 1s<sup>2</sup>2s5p(19), 1s<sup>2</sup>2s5d(20), 1s<sup>2</sup>2s5f(21), 1s<sup>2</sup>2s5g(22),  
 1s<sup>2</sup>2p5s(23), 1s<sup>2</sup>2p5p(24), 1s<sup>2</sup>2p5d(25), 1s<sup>2</sup>2p5f(26), 1s<sup>2</sup>2p5g(27), 1s2s<sup>2</sup>2p(28), 1s<sup>2</sup>3s<sup>2</sup>(29),  
 1s<sup>2</sup>3p<sup>2</sup>(30), 1s<sup>2</sup>3d<sup>2</sup>(31)

Au<sup>+74</sup>

1s<sup>2</sup>2s<sup>2</sup>2p(1), 1s<sup>2</sup>2s2p<sup>2</sup>(2), 1s<sup>2</sup>2p<sup>3</sup>(3), 1s<sup>2</sup>2s<sup>2</sup>3s(4), 1s<sup>2</sup>2s<sup>2</sup>3p(5), 1s<sup>2</sup>2s<sup>2</sup>3d(6), 1s<sup>2</sup>2s2p3s(7),  
 1s<sup>2</sup>2s2p3p(8), 1s<sup>2</sup>2s2p3d(9), 1s<sup>2</sup>2s<sup>2</sup>4s(10), 1s<sup>2</sup>2s<sup>2</sup>4p(11), 1s<sup>2</sup>2s<sup>2</sup>4d(12), 1s<sup>2</sup>2s<sup>2</sup>4f(13), 1s<sup>2</sup>2s2p4s(14),  
 1s<sup>2</sup>2s2p4p(15), 1s<sup>2</sup>2s2p4d(16), 1s<sup>2</sup>2s3d<sup>2</sup>(17), 1s<sup>2</sup>2p<sup>2</sup>3s(18), 1s<sup>2</sup>2p<sup>2</sup>3p(19), 1s<sup>2</sup>2p<sup>2</sup>3d(20), 1s<sup>2</sup>2p<sup>2</sup>4s(21),  
 1s<sup>2</sup>2p<sup>2</sup>4p(22), 1s<sup>2</sup>s<sup>2</sup>2p<sup>2</sup>(23), 1s<sup>2</sup>s<sup>2</sup>2p3p(24), 1s<sup>2</sup>s<sup>2</sup>2p3d(25)

Au<sup>+73</sup>

1s<sup>2</sup>2s<sup>2</sup>2p<sup>2</sup>(1), 1s<sup>2</sup>2s2p<sup>3</sup>(2), 1s<sup>2</sup>2p<sup>4</sup>(3), 1s<sup>2</sup>2s<sup>2</sup>2p3s(4), 1s<sup>2</sup>2s<sup>2</sup>2p3p(5), 1s<sup>2</sup>2s<sup>2</sup>2p3d(6),  
 1s<sup>2</sup>2s<sup>2</sup>2p4s(7), 1s<sup>2</sup>2s<sup>2</sup>2p4p(8), 1s<sup>2</sup>2s<sup>2</sup>2p4d(9), 1s<sup>2</sup>2s<sup>2</sup>2p4f(10), 1s<sup>2</sup>2s2p<sup>2</sup>3s(11), 1s<sup>2</sup>2s2p<sup>2</sup>3p(12),  
 1s<sup>2</sup>2s2p<sup>2</sup>3d(13), 1s<sup>2</sup>2s2p<sup>2</sup>4s(14), 1s<sup>2</sup>2s2p<sup>2</sup>4p(15), 1s<sup>2</sup>2s2p<sup>2</sup>4d(16), 1s<sup>2</sup>2s<sup>2</sup>2p<sup>3</sup>(17)

Au<sup>+72</sup>

1s<sup>2</sup>2s<sup>2</sup>2p<sup>3</sup>(1), 1s<sup>2</sup>2s2p<sup>4</sup>(2), 1s<sup>2</sup>2s<sup>2</sup>2p<sup>2</sup>3s(3), 1s<sup>2</sup>2s<sup>2</sup>2p<sup>2</sup>3p(4), 1s<sup>2</sup>2s<sup>2</sup>2p<sup>2</sup>3d(5), 1s<sup>2</sup>2s<sup>2</sup>2p<sup>2</sup>4s(6),  
 1s<sup>2</sup>2s<sup>2</sup>2p<sup>2</sup>4p(7), 1s<sup>2</sup>2s<sup>2</sup>2p<sup>2</sup>4d(8), 1s<sup>2</sup>2s<sup>2</sup>2p<sup>2</sup>4f(9), 1s<sup>2</sup>2p<sup>5</sup>(10), 1s<sup>2</sup>2s2p<sup>3</sup>3s(11), 1s<sup>2</sup>2s2p<sup>3</sup>3p(12),  
 1s<sup>2</sup>2s2p<sup>3</sup>3d(13), 1s<sup>2</sup>2s2p<sup>4</sup>(14)

Au<sup>+71</sup>

1s<sup>2</sup>2s<sup>2</sup>2p<sup>4</sup>(1), 1s<sup>2</sup>2s2p<sup>5</sup>(2), 1s<sup>2</sup>2p<sup>6</sup>(3), 1s<sup>2</sup>2s<sup>2</sup>2p<sup>3</sup>3s(4), 1s<sup>2</sup>2s<sup>2</sup>2p<sup>3</sup>3p(5), 1s<sup>2</sup>2s<sup>2</sup>2p<sup>3</sup>3d(6),  
 1s<sup>2</sup>2s<sup>2</sup>2p<sup>3</sup>4s(7), 1s<sup>2</sup>2s<sup>2</sup>2p<sup>3</sup>4p(8), 1s<sup>2</sup>2s<sup>2</sup>2p<sup>3</sup>4d(9), 1s<sup>2</sup>2s<sup>2</sup>2p<sup>3</sup>4f(10), 1s<sup>2</sup>2s2p<sup>4</sup>3s(11), 1s<sup>2</sup>2s2p<sup>4</sup>3p(12),  
 1s<sup>2</sup>2s2p<sup>4</sup>3d(13), 1s<sup>2</sup>2s2p<sup>4</sup>4s(14), 1s<sup>2</sup>2s2p<sup>4</sup>4p(15), 1s<sup>2</sup>2s2p<sup>4</sup>4d(16), 1s<sup>2</sup>2s<sup>2</sup>2p<sup>2</sup>3s<sup>2</sup>(17), 1s2s<sup>2</sup>2p<sup>5</sup>(18)

Au<sup>+70</sup>

1s<sup>2</sup>2s<sup>2</sup>2p<sup>5</sup>(1), 1s<sup>2</sup>2s2p<sup>6</sup>(2), 1s<sup>2</sup>2s<sup>2</sup>2p<sup>4</sup>3s(3), 1s<sup>2</sup>2s<sup>2</sup>2p<sup>4</sup>3p(4), 1s<sup>2</sup>2s<sup>2</sup>2p<sup>4</sup>3d(5), 1s<sup>2</sup>2s<sup>2</sup>2p<sup>4</sup>4s(6),  
 1s<sup>2</sup>2s<sup>2</sup>2p<sup>4</sup>4p(7), 1s<sup>2</sup>2s<sup>2</sup>2p<sup>4</sup>4d(8), 1s<sup>2</sup>2s<sup>2</sup>2p<sup>4</sup>4f(9), 1s<sup>2</sup>2s2p<sup>5</sup>3s(10), 1s<sup>2</sup>2s2p<sup>5</sup>3p(11), 1s<sup>2</sup>2s2p<sup>5</sup>3d(12),  
 1s<sup>2</sup>2s2p<sup>5</sup>4s(13), 1s<sup>2</sup>2s2p<sup>5</sup>4p(14), 1s<sup>2</sup>2s2p<sup>5</sup>4d(15), 1s<sup>2</sup>2s<sup>2</sup>2p<sup>6</sup>(16)

The configurations are numbered, within parentheses, for convenience.

energies compared with experimental ones, and then the same set of configurations was used for the gold ion. Uncertainties remain with the procedure since these gold ions are highly ionized requiring additional optimization due to strong nuclear force.

The 1s–2p transitions for each ionic state of gold ( $Z = 79$ ), H-like ( $N_e = 1$ ), He-like ( $N_e = 2$ ), Li-like ( $N_e = 3$ ), etc. are presented in Table 2. The transition energies are given both in Å and keV. The configuration numbers  $C_i$ ,  $C_j$  of an ion represent their positions in the set in Table 1 used in calculations. The corresponding configurations are written explicitly above the 1s–2p transitions of the ion. Table 2 shows that gold K<sub>z</sub> lines

Table 2

*f*, *S*, and *A*-values for the K<sub>z</sub> 1s–2p transitions in gold

Z	N <sub>e</sub>	SLπC <sub>i</sub>	SLπC <sub>j</sub>	<i>g<sub>i</sub></i>	<i>g<sub>j</sub></i>	λ (Å)	E (keV)	<i>E<sub>i</sub></i> (Ry)	<i>E<sub>j</sub></i> (Ry)	<i>f<sub>ij</sub></i>	<i>S</i>	<i>A<sub>ji</sub></i> (s <sup>-1</sup> )
<b>Au<sup>+78</sup> : C<sub>i</sub>(1) = 1s, C<sub>j</sub>(3) = 2p</b>												
79	1	2Se 1	2Po 3	2	2	0.1800	68.880	0.00	5050.86	9.84E – 02	1.17E – 04	2.02E + 16
79	1	2Se 1	2Po 3	2	4	0.1760	70.446	0.00	5191.18	1.94E – 01	2.24E – 04	2.10E + 16
<b>Au<sup>+77</sup> : C<sub>i</sub>(1) = 1s<sup>2</sup>, C<sub>j</sub>(3) = 1s2p</b>												
79	2	1Se 1	1Po 3	1	3	0.1780	69.654	0.00	5121.71	3.93E – 01	2.30E – 04	2.76E + 16
79	2	1Se 1	3Po 3	1	3	0.1830	67.751	0.00	4984.28	1.85E – 01	1.11E – 04	1.23E + 16
<b>Au<sup>+76</sup> : C<sub>i</sub>(1) = 1s<sup>2</sup>2s, C<sub>j</sub>(11) = 1s2s2p</b>												
79	3	2Se 1	2Po11	2	2	0.1810	68.500	0.00	5029.12	5.03E – 02	6.00E – 05	1.02E + 16
79	3	2Se 1	2Po11	2	4	0.1780	69.654	0.00	5115.67	1.76E – 01	2.06E – 04	1.85E + 16
79	3	2Se 1	2Po11	2	2	0.1780	69.654	0.00	5119.36	1.23E – 01	1.44E – 04	2.59E + 16
79	3	2Se 1	2Po11	2	4	0.1770	70.048	0.00	5160.38	8.37E – 02	9.73E – 05	8.95E + 15
79	3	2Se 1	4Po11	2	2	0.1830	67.751	0.00	4979.31	1.42E – 02	1.71E – 05	2.82E + 15
79	3	2Se 1	4Po11	2	4	0.1830	67.751	0.00	4982.99	1.16E – 01	1.39E – 04	1.15E + 16
<b>Au<sup>+75</sup> : C<sub>i</sub>(1) = 1s<sup>2</sup>2s<sup>2</sup>, C<sub>j</sub>(28) = 1s2s<sup>2</sup>2p</b>												
79	4	1Se 1	1Po28	1	3	0.1780	69.654	4.11	5131.82	3.46E – 01	2.02E – 04	2.43E + 16
79	4	1Se 1	3Po28	1	3	0.1820	68.123	4.11	5009.60	1.67E – 01	1.00E – 04	1.12E + 16
<b>Au<sup>+74</sup> : C<sub>i</sub>(1) = 1s<sup>2</sup>2s<sup>2</sup>2p, C<sub>j</sub>(23) = 1s2s<sup>2</sup>2p<sup>2</sup></b>												
79	5	2Po 1	2De23	2	4	0.1780	69.654	0.00	5108.53	5.02E – 04	5.89E – 07	5.26E + 13
79	5	2Po 1	2De23	4	4	0.1830	67.751	128.19	5108.53	1.95E – 02	4.69E – 05	3.88E + 15
79	5	2Po 1	2De23	4	6	0.1830	67.751	128.19	5111.67	9.37E – 02	2.26E – 04	1.25E + 16
79	5	2Po 1	2Pe23	2	2	0.1780	69.654	0.00	5112.71	1.24E – 01	1.45E – 04	2.59E + 16
79	5	2Po 1	2Pe23	4	2	0.1830	67.751	128.19	5112.71	3.12E – 02	7.52E – 05	1.25E + 16
79	5	2Po 1	2Pe23	2	4	0.1740	71.255	0.00	5240.80	1.16E – 05	1.33E – 08	1.29E + 12
79	5	2Po 1	2Pe23	4	4	0.1780	69.654	128.19	5240.80	1.79E – 01	4.20E – 04	3.76E + 16
79	5	2Po 1	2Se23	2	2	0.1740	71.255	0.00	5242.87	1.07E – 05	1.23E – 08	2.37E + 12
79	5	2Po 1	2Se23	4	2	0.1780	69.654	128.19	5242.87	4.39E – 02	1.03E – 04	1.84E + 16
79	5	2Po 1	4Pe23	2	2	0.1830	67.751	0.00	4986.11	8.70E – 02	1.05E – 04	1.74E + 16
79	5	2Po 1	4Pe23	4	2	0.1880	65.949	128.19	4986.11	9.67E – 05	2.39E – 07	3.67E + 13
79	5	2Po 1	4Pe23	2	4	0.1780	69.654	0.00	5114.15	2.36E – 01	2.77E – 04	2.48E + 16
79	5	2Po 1	4Pe23	4	4	0.1830	67.751	128.19	5114.15	4.22E – 02	1.02E – 04	8.43E + 15
79	5	2Po 1	4Pe23	4	6	0.1780	69.654	128.19	5236.84	4.66E – 02	1.09E – 04	6.51E + 15
<b>Au<sup>+73</sup> : C<sub>i</sub>(1) = 1s<sup>2</sup>2s<sup>2</sup>2p<sup>2</sup>, C<sub>j</sub>(17) = 1s2s<sup>2</sup>2p<sup>3</sup></b>												
79	6	3Pe 1	3Po17	3	5	0.1824	67.974	124.57	5120.67	6.60E – 02	1.19E – 04	7.94E + 15
79	6	3Pe 1	3Po17	5	5	0.1872	66.231	252.95	5120.67	3.02E – 05	9.30E – 08	5.74E + 12
79	6	3Pe 1	3Po17	1	3	0.1778	69.732	0.00	5123.80	3.35E – 01	1.96E – 04	2.35E + 16
79	6	3Pe 1	3Po17	3	3	0.1823	68.011	124.57	5123.80	1.34E – 02	2.42E – 05	2.70E + 15
79	6	3Pe 1	3Po17	5	3	0.1871	66.266	252.95	5123.80	3.31E – 05	1.02E – 07	1.05E + 13
79	6	3Pe 1	3Do17	5	7	0.1828	67.825	252.95	5238.57	7.76E – 02	2.33E – 04	1.11E + 16
79	6	3Pe 1	3So17	1	3	0.1739	71.296	0.00	5239.72	2.07E – 05	1.19E – 08	1.52E + 12
79	6	3Pe 1	3So17	3	3	0.1782	69.576	124.57	5239.72	1.42E – 01	2.49E – 04	2.98E + 16
79	6	3Pe 1	3So17	5	3	0.1827	67.862	252.95	5239.72	3.29E – 02	9.89E – 05	1.09E + 16
79	6	1De 1	1Do17	5	5	0.1782	69.576	126.79	5241.67	1.54E – 01	4.51E – 04	3.23E + 16
79	6	3Pe 1	3Po17	3	1	0.1781	69.615	124.57	5241.77	2.75E – 02	4.83E – 05	1.73E + 16
79	6	1De 1	1Po17	5	3	0.1781	69.615	126.79	5243.29	4.27E – 02	1.25E – 04	1.50E + 16
79	6	1Se 1	1Po17	1	3	0.1828	67.825	257.25	5243.29	1.65E – 01	9.94E – 05	1.10E + 16
79	6	3Pe 1	3Do17	3	5	0.1741	71.214	124.57	5357.52	2.37E – 07	4.07E – 10	3.12E + 10
79	6	3Pe 1	3Do17	5	5	0.1785	69.459	252.95	5357.52	8.70E – 02	2.56E – 04	1.82E + 16
79	6	3Pe 1	3Do17	1	3	0.1700	72.932	0.00	5360.51	6.93E – 08	3.88E – 11	5.33E + 09
79	6	3Pe 1	3Do17	3	3	0.1740	71.255	124.57	5360.51	1.35E – 05	2.32E – 08	2.97E + 12
79	6	3Pe 1	3Do17	5	3	0.1784	69.498	252.95	5360.51	8.44E – 02	2.48E – 04	2.95E + 16
79	6	1De 1	3Po17	5	5	0.1825	67.937	126.79	5120.67	3.78E – 02	1.13E – 04	7.56E + 15
79	6	1De 1	3Po17	5	3	0.1824	67.974	126.79	5123.80	3.94E – 02	1.18E – 04	1.32E + 16

Table 2 (continued)

Z	N <sub>e</sub>	SLπC <sub>i</sub>	SLπC <sub>j</sub>	g <sub>i</sub>	g <sub>j</sub>	λ (Å)	E (keV)	E <sub>i</sub> (Ry)	E <sub>j</sub> (Ry)	f <sub>ij</sub>	S	A <sub>ji</sub> (s <sup>-1</sup> )
79	6	1Se 1	3Po17	1	3	0.1873	66.196	257.25	5123.80	4.78E – 05	2.95E – 08	3.03E + 12
79	6	3Pe 1	5So17	3	5	0.1783	69.537	124.57	5235.09	4.70E – 02	8.28E – 05	5.92E + 15
79	6	1De 1	5So17	5	5	0.1784	69.498	126.79	5235.09	1.83E – 03	5.37E – 06	3.83E + 14
79	6	3Pe 1	5So17	5	5	0.1829	67.788	252.95	5235.09	1.91E – 02	5.74E – 05	3.80E + 15
79	6	1De 1	3Do17	5	7	0.1783	69.537	126.79	5238.57	4.05E – 02	1.19E – 04	6.07E + 15
79	6	1De 1	3So17	5	3	0.1782	69.576	126.79	5239.72	1.76E – 02	5.16E – 05	6.15E + 15
79	6	1Se 1	3So17	1	3	0.1829	67.788	257.25	5239.72	6.53E – 08	3.93E – 11	4.34E + 09
79	6	3Pe 1	1Do17	3	5	0.1781	69.615	124.57	5241.67	2.43E – 02	4.28E – 05	3.07E + 15
79	6	3Pe 1	1Do17	5	5	0.1827	67.862	252.95	5241.67	3.60E – 02	1.08E – 04	7.20E + 15
79	6	3Pe 1	1Po17	1	3	0.1738	71.337	0.00	5243.29	1.79E – 05	1.02E – 08	1.31E + 12
79	6	3Pe 1	1Po17	3	3	0.1780	69.654	124.57	5243.29	1.29E – 02	2.27E – 05	2.72E + 15
79	6	3Pe 1	1Po17	5	3	0.1826	67.899	252.95	5243.29	3.92E – 06	1.18E – 08	1.31E + 12
79	6	1De 1	3Do17	5	5	0.1742	71.174	126.79	5357.52	6.88E – 06	1.97E – 08	1.51E + 12
79	6	1De 1	3Do17	5	3	0.1741	71.214	126.79	5360.51	9.72E – 08	2.78E – 10	3.56E + 10
79	6	1Se 1	3Do17	1	3	0.1786	69.420	257.25	5360.51	1.75E – 01	1.03E – 04	1.22E + 16
<b>Au<sup>+72</sup> : C<sub>i</sub>(1) = 1s<sup>2</sup>s<sup>2</sup>2p<sup>3</sup>, C<sub>j</sub>(14) = 1s<sup>2</sup>s<sup>2</sup>2p<sup>4</sup></b>												
79	7	4So 1	4Pe14	4	6	0.1830	67.751	122.78	5103.20	6.40E – 02	1.54E – 04	8.50E + 15
79	7	2Do 1	2Pe14	4	4	0.1784	69.498	0.00	5107.01	1.65E – 01	3.88E – 04	3.46E + 16
79	7	2Do 1	2Pe14	6	4	0.1829	67.788	125.56	5107.01	4.22E – 02	1.53E – 04	1.26E + 16
79	7	2Po 1	2Pe14	2	4	0.1830	67.751	128.69	5107.01	1.81E – 06	2.18E – 09	1.80E + 11
79	7	2Po 1	2Pe14	4	4	0.1877	66.054	252.05	5107.01	5.36E – 05	1.32E – 07	1.01E + 13
79	7	2Po 1	2Se14	2	2	0.1830	67.751	128.69	5108.93	7.88E – 02	9.49E – 05	1.57E + 16
79	7	2Po 1	2Se14	4	2	0.1876	66.090	252.05	5108.93	1.70E – 05	4.19E – 08	6.43E + 12
79	7	2Do 1	2De14	4	4	0.1746	71.010	0.00	5219.54	6.75E – 06	1.55E – 08	1.48E + 12
79	7	2Do 1	2De14	6	4	0.1789	69.304	125.56	5219.54	4.29E – 03	1.52E – 05	1.34E + 15
79	7	2Po 1	2De14	2	4	0.1790	69.265	128.69	5219.54	2.14E – 04	2.52E – 07	2.22E + 13
79	7	2Po 1	2De14	4	4	0.1834	67.603	252.05	5219.54	1.77E – 02	4.29E – 05	3.52E + 15
79	7	2Do 1	2De14	4	6	0.1745	71.051	0.00	5222.51	2.08E – 06	4.79E – 09	3.04E + 11
79	7	2Do 1	2De14	6	6	0.1788	69.342	125.56	5222.51	7.97E – 02	2.82E – 04	1.66E + 16
79	7	2Po 1	2De14	4	6	0.1833	67.640	252.05	5222.51	8.37E – 02	2.02E – 04	1.11E + 16
79	7	2Do 1	2Pe14	4	2	0.1745	71.051	0.00	5223.33	8.68E – 07	1.99E – 09	3.80E + 11
79	7	2Po 1	2Pe14	2	2	0.1789	69.304	128.69	5223.33	5.89E – 02	6.94E – 05	1.23E + 16
79	7	2Po 1	2Pe14	4	2	0.1833	67.640	252.05	5223.33	2.74E – 02	6.62E – 05	1.09E + 16
79	7	4So 1	4Pe14	4	4	0.1786	69.420	122.78	5224.79	1.04E – 02	2.44E – 05	2.17E + 15
79	7	4So 1	4Pe14	4	2	0.1746	71.010	122.78	5341.23	5.52E – 06	1.27E – 08	2.42E + 12
79	7	2Do 1	4Pe14	4	6	0.1786	69.420	0.00	5103.20	4.30E – 02	1.01E – 04	6.00E + 15
79	7	2Do 1	4Pe14	6	6	0.1831	67.714	125.56	5103.20	3.54E – 02	1.28E – 04	7.05E + 15
79	7	2Po 1	4Pe14	4	6	0.1878	66.019	252.05	5103.20	1.19E – 05	2.95E – 08	1.50E + 12
79	7	4So 1	2Pe14	4	4	0.1828	67.825	122.78	5107.01	1.67E – 02	4.02E – 05	3.33E + 15
79	7	2Do 1	2Se14	4	2	0.1784	69.498	0.00	5108.93	4.09E – 02	9.60E – 05	1.71E + 16
79	7	4So 1	2Se14	4	2	0.1828	67.825	122.78	5108.93	1.38E – 06	3.32E – 09	5.51E + 11
79	7	4So 1	2De14	4	4	0.1788	69.342	122.78	5219.54	7.95E – 02	1.87E – 04	1.66E + 16
79	7	4So 1	2De14	4	6	0.1787	69.381	122.78	5222.51	7.96E – 03	1.87E – 05	1.11E + 15
79	7	4So 1	2Pe14	4	2	0.1787	69.381	122.78	5223.33	6.82E – 02	1.60E – 04	2.85E + 16
79	7	2Do 1	4Pe14	4	4	0.1744	71.092	0.00	5224.79	1.07E – 05	2.45E – 08	2.34E + 12
79	7	2Do 1	4Pe14	6	4	0.1787	69.381	125.56	5224.79	8.58E – 02	3.03E – 04	2.69E + 16
79	7	2Po 1	4Pe14	2	4	0.1788	69.342	128.69	5224.79	1.13E – 01	1.33E – 04	1.17E + 16
79	7	2Po 1	4Pe14	4	4	0.1833	67.640	252.05	5224.79	3.82E – 02	9.21E – 05	7.58E + 15
79	7	2Do 1	4Pe14	4	2	0.1706	72.675	0.00	5341.23	1.76E – 08	3.96E – 11	8.08E + 09
79	7	2Po 1	4Pe14	2	2	0.1748	70.929	128.69	5341.23	8.55E – 06	9.84E – 09	1.87E + 12
79	7	2Po 1	4Pe14	4	2	0.1791	69.226	252.05	5341.23	8.54E – 02	2.01E – 04	3.55E + 16
<b>Au<sup>+71</sup> : C<sub>i</sub>(1) = 1s<sup>2</sup>s<sup>2</sup>2p<sup>4</sup>, C<sub>j</sub>(18) = 1s<sup>2</sup>s<sup>2</sup>2p<sup>5</sup></b>												
79	8	3Pe 1	3Po18	5	5	0.1780	69.654	0.00	5106.65	8.07E – 02	2.37E – 04	1.69E + 16
79	8	3Pe 1	3Po18	3	5	0.1830	67.751	121.16	5106.65	6.49E – 02	1.17E – 04	7.77E + 15
79	8	1Se 1	1Po18	1	3	0.1780	69.654	4.17	5109.53	1.62E – 01	9.52E – 05	1.13E + 16

Table 2 (continued)

Z	N <sub>e</sub>	SLπC <sub>i</sub>	SLπC <sub>j</sub>	g <sub>i</sub>	g <sub>j</sub>	λ (Å)	E (keV)	E <sub>i</sub> (Ry)	E <sub>j</sub> (Ry)	f <sub>ij</sub>	S	A <sub>ji</sub> (s <sup>-1</sup> )
79	8	1De 1	1Po18	5	3	0.1830	67.751	123.39	5109.53	3.86E – 02	1.16E – 04	1.28E + 16
79	8	3Pe 1	3Po18	3	1	0.1790	69.265	121.16	5219.64	5.32E – 02	9.40E – 05	3.33E + 16
79	8	3Pe 1	3Po18	5	3	0.1750	70.848	0.00	5221.14	4.23E – 06	1.22E – 08	1.54E + 12
79	8	3Pe 1	3Po18	3	3	0.1790	69.265	121.16	5221.14	2.59E – 02	4.58E – 05	5.42E + 15
79	8	3Pe 1	3Po18	1	3	0.1830	67.751	246.25	5221.14	1.62E – 01	9.76E – 05	1.07E + 16
79	8	1De 1	3Po18	5	5	0.1830	67.751	123.39	5106.65	3.75E – 02	1.13E – 04	7.49E + 15
79	8	3Pe 1	1Po18	5	3	0.1780	69.654	0.00	5109.53	7.83E – 02	2.30E – 04	2.74E + 16
79	8	3Pe 1	1Po18	3	3	0.1830	67.751	121.16	5109.53	1.37E – 02	2.47E – 05	2.73E + 15
79	8	3Pe 1	1Po18	1	3	0.1870	66.302	246.25	5109.53	6.05E – 05	3.73E – 08	3.83E + 12
79	8	1Se 1	3Po18	1	3	0.1750	70.848	4.17	5221.14	1.67E – 05	9.61E – 09	1.22E + 12
79	8	1De 1	3Po18	5	3	0.1790	69.265	123.39	5221.14	8.23E – 02	2.42E – 04	2.86E + 16
$\text{Au}^{+70} : C_i(1) = 1s^2 2s^2 2p^5, C_j(16) = 1s 2s^2 2p^6$												
79	9	2Po 1	2Se16	4	2	0.1790	69.265	0.00	5088.63	8.22E – 02	1.94E – 04	3.42E + 16
79	9	2Po 1	2Se16	2	2	0.1840	67.383	123.71	5088.63	8.06E – 02	9.74E – 05	1.59E + 16

While transition energies are in Å and keV, the individual level energies, relative to the ground level, are in Ry. The configuration numbers ( $C_{ij}$ ) for the gold ionic states correspond to the sets of Table 1.

due to 1s–2p transitions are in the hard X-ray region from 66 to 72.68 keV, and wavelength range from 0.188 to 0.1706 Å.

For ions, such as H-like, He-like, Be-like and F-like Au, there are two 1s–2p transitions and each of them has strong transition probability of order  $10^{16} \text{ s}^{-1}$  (Table 2). However, for B-like, C-like, N-like, and O-like ions, with more complex 2p configurations, the total number of 1s–2p transition changes due to formation of larger number of fine structure J-levels before and after the transition. This increases the number of allowed E1 transitions. For example, for C-like Au,  $\text{Au}^{+73}$ , the ground configuration  $1s^2 2s^2 2p^2$  has three terms  $^3P$ ,  $^1D$ ,  $^1S_0$ , and the excited configuration  $1s^2 2s^2 2p^3$  has six terms  $^5S^o$ ,  $^3S^o$ ,  $^3D^o$ ,  $^1D^o$ ,  $^3P^o$ ,  $^1P^o$ . Each term corresponds to one or more J-levels. Hence, the number of E1 transitions among the 1s–2p levels of  $\text{Au}^{+73}$  increases to 35.

The E1 transitions are of dipole allowed where the spin does not change ( $\Delta S = 0$ ), or intercombination type, where spin changes ( $\Delta S \neq 0$ ). Typically the intercombination transitions are weaker than those of same-spin-multiplets. However there are exceptions, as seen for gold ions. While most of the same-spin-multiplets transitions are strong with a large A-value of  $\sim 10^{16} \text{ s}^{-1}$ , there are some that are weak with A-values  $\sim 10^{12} \text{ s}^{-1}$  or less. The same-spin-multiplets transition,  $^3P_1^e - ^3D_2^o$  in  $\text{Au}^{+73}$ , is a very weak transition with an A-value as low as,  $10^9 \text{ s}^{-1}$ . Again, the intercombination transition,  $1s^2 2s^2 (^1S_0) - 1s 2s^2 2p (^3P_1^o)$  of Be-like Au, is strong with the rate as high as  $10^{16} \text{ s}^{-1}$ . We note that to obtain an estimate of the intensity of a broadened 1s–2p line, such as in high density plasmas, all the relevant oscillator strengths for transitions contributing to the feature can be summed up.

To our knowledge, the energies and oscillator strengths of K<sub>z</sub> lines of these ions are not in the published literature except for a few ions, H- and He-like Au. To benchmark the present results, we have employed two accurate approaches, the relativistic multi-configuration Dirac–Fock method using the code GRASP [12], and relativistic coupled cluster (RCC) approximation [13], to calculate the A-values of 1s–2p transitions of a few ionic states of Au. Table 3 presents these comparisons along with those currently available.

For H-like Au,  $\text{Au}^{+78}$ , the transition energies for K<sub>z1</sub> line ( $1s^2 S_{3/2} - 2p^2 P_{1/2}^o$ ) and K<sub>z2</sub> line ( $1s^2 S_{1/2} - 2p^2 P_{1/2}^o$ ) of H-like Au were measured to be 66.991 and 68.805 keV [11], respectively. As seen in Table 3, present values for these transitions are close to the measured values as well as to those from elaborate calculations of using the relativistic Dirac theory with higher-order radiation such as electric and magnetic multipole contributions by Pal'chikav [14]. Present A-values differ from those by Pal'chikav by about 20% for K<sub>z2</sub>, and by 6% for K<sub>z1</sub> transition.

For He-like Au,  $\text{Au}^{+77}$ , we compare the transitions with those by Plante et al. [15] calculated using relativistic many body perturbative theory that includes both relativistic corrections as well as QED effects. We also compute the A-values using GRASP. As Table 3 shows, transition energies from SS agree very well

Table 3

Comparison of the present values with others

Ion	Transition	$E_{ij}$ (keV)	$f$	$A$ ( $s^{-1}$ )
$Au^{+78}$	$^2P_{1/2}^o - ^2S_{1/2}$	66.991 <sup>a</sup> , 68.88 <sup>p1</sup> , 69.317 <sup>b</sup>		2.02e + 16 <sup>p1</sup> , 2.53e + 16 <sup>b</sup>
$Au^{+78}$	$^2P_{3/2}^o - ^2S_{1/2}$	68.805 <sup>a</sup> , 70.45 <sup>p1</sup> , 71.556 <sup>b</sup>		2.10e + 16 <sup>p1</sup> , 2.24e + 16 <sup>b</sup>
$Au^{+77}$	$^1P_1^o - ^1S_0$	69.654 <sup>p1</sup> , 70.40 <sup>c</sup>		2.76e + 16 <sup>p1</sup> , 2.75e + 16 <sup>p2</sup> , 2.85e + 16 <sup>c</sup>
$Au^{+77}$	$^3P_1^o - ^1S_0$	67.751 <sup>p1</sup> , 68.220 <sup>c</sup>		1.23e + 16 <sup>p1</sup> , 1.615e + 16 <sup>p2</sup> , 1.58e + 16 <sup>c</sup>
$Au^{+76}$	$^2P_{1/2}^o - ^2S_{1/2}$	69.654 <sup>p1</sup>	0.123 <sup>p1</sup> , 0.13 <sup>d</sup>	
$Au^{+75}$	$^1P_1^o - ^1S_0$	69.654 <sup>p1</sup>		2.43e + 16 <sup>p1</sup> , 2.63e + 16 <sup>p2</sup>
$Au^{+75}$	$^3P_1^o - ^1S_0$	68.123 <sup>p1</sup>		1.12e + 16 <sup>p1</sup> , 1.57e + 16 <sup>p2</sup>
$Au^{+70}$	$^2P_{1/2}^o - ^2S_{1/2}$	67.383 <sup>p1</sup> , 67.764 <sup>p3</sup>		1.59e + 16 <sup>p1</sup> , 2.16e + 16 <sup>p3</sup>
$Au^{+70}$	$^2P_{3/2}^o - ^2S_{1/2}$	69.265 <sup>p1</sup> , 69.667 <sup>p3</sup>		3.42e + 16 <sup>p1</sup> , 2.31e + 16 <sup>p3</sup>

Present values are p1 from SUPERSTRUCTURE (SS), p2 from GRASP, p3 from relativistic coupled cluster method.

<sup>a</sup>Deslattes and Kessler-expt [11].<sup>b</sup>Pal'chikov [14].<sup>c</sup>Plane et al. [15].<sup>d</sup>Safronova and Safronova [16].

with those by Plante et al. All  $A$ -values for the resonant line  $1s^2(^1S_0) - 1s2p(^1P_1^o)$  from SS (p1), GRASP (p2), and RMBPT [15] agree very well. However, SS-value for the intercombination transition is over 20% below those from GRASP and RMBPT.

For Li-like Au,  $Au^{76+}$ , we compare the present  $f$ -value for the transition  $1s2s2p(^2P_{1/2}^o) - 1s^22s(^2S_{1/2})$  with that by Safronova and Safronova (2004) using relativistic many-body perturbation theory that includes the Breit interaction, and we find agreement within 6%.

For Be-like Au,  $Au^{75+}$ , we make comparison between SS and GRASP. While we find good agreement within 8% for the same-spin dipole transition, SS-value is 29% lower for the intercombination transition. Finally, we compare  $A$ -values for the F-like Au,  $Au^{70}$ , between SS and RCC (p3). Although the energies show very good agreement for both transitions,  $A$ -values from SS differ by 30% from those from RCC.

Based on all these comparisons, it may be concluded that present results from SS have good agreement with other approximations for the same-spin dipole-allowed transitions. However, they are lower than for the intercombination transitions by about 30%. Present results do not consider higher order relativistic effects and could be the reason for the differences. Higher order relativistic contributions appear to be more important than configuration interaction with higher  $Z$  ions. Although not highly accurate for all transitions, present results should provide good estimation for 1s–2p transitions in all ionic states of gold considered herein.

#### 4. Conclusion

The  $f$ ,  $S$ ,  $A$ -values are presented for  $K_\alpha$  lines of gold ions, from H-like  $Au^{+78}$  to F-like  $Au^{+70}$ . The energies of these lines are in the hard X-ray region with a wavelength range of 0.1706 to 0.1888 Å. The number of 1s–2p transitions varies from the  $K_\alpha$  doublets to a much larger number depending on the number of active 2p electrons, and resulting fine structure levels for the transitional configurations. While same-spin multiplet transitions show good agreement with other more accurate approaches, higher order relativistic contributions appear to be more important for the intercombination transitions. Until highly accurate values are available, the present results should be reasonably accurate for various applications in plasma diagnostics and modeling of high energy-temperature laboratory sources in several areas.

Although only the 1s–2p transitions are reported here, a large number of transitions, including electric quadrupole and magnetic dipole transitions among all the configurations in Table 1 are also available from the first author.

## Acknowledgments

This work was partially supported by a Large Interdisciplinary Grant award from the Ohio State University. The computational work was carried out on the Cray X1 and Itanium 4 cluster at the Ohio Supercomputer Center in Columbus Ohio. C. Sur acknowledges Dr. Rajat Chaudhuri for helpful discussions and developing codes for relativistic coupled cluster calculations.

## References

- [1] Kishimoto S, et al. Observation of nuclear excitation by electron transition in  $^{197}\text{Au}$  with synchrotron X-rays and an avalanche photodiode. *Phys Rev Lett* 2000;85:1831–4.
- [2] Chien CC, et al. Synchrotron X-Ray synthesized gold nanoparticles for tumor therapy, synchrotron radiation instrumentation: ninth international conference on synchrotron radiation instrumentation. *AIP Conf Proc* 2007;879:1908–11.
- [3] Hainfeld J, et al. The use of gold nanoparticles to enhance radiotherapy in mice. *Phys Med Biol* 2004;49:N309–15.
- [4] Seely JF, Back CA, Constantin C, Lee RW, Chung H-K, Hudson LT, et al. Krypton K-shell X-ray spectra recorded by the HENEX spectrometer. *JQSRT* 2005;99:572–83.
- [5] Hudson LT, Atkin R, Back CA, Henins A, Holland GE, Seely JF, et al. X-ray spectroscopy at next-generation inertial confinement fusion sources: anticipating needs and challenges. *Rad Phys Chem* 2006;75:1784–98.
- [6] Eissner W, Jones M, Nussbaumer H. Techniques for the calculation of atomic structures and radiative data including relativistic corrections. *Comput Phys Commun* 1974;8:270–306.
- [7] Nahar SN, Eissner W, Chen GX, Pradhan AK. Atomic data from the iron project—LIII, relativistic allowed and forbidden transition probabilities for Fe XVII. *Astron Astrophys* 2003;408:789–801.
- [8] Eissner W, Zeippen CJ. Interference between ordinary and higher-order amplitudes in O II magnetic dipole transitions. *J Phys B* 1981;14:2125–37.
- [9] Eissner W. In: Wilson S, et al., editors. The effects of relativity on atoms, molecules, and the solid state. New York: Plenum Press; 1991. p. 55.
- [10] Nahar SN. Atomic data from the iron project-LXI, Radiative E1, E2, E3, and M1 transition probabilities for Fe I. *Astron Astrophys* 2006;448:779–85.
- [11] Desslattes RD, Kessler Jr EG. Atomic inner shell physics. New York: Plenum Press; 1985. p. 181–235.
- [12] Parpia FA, Froese Fischer C, Grant IP. GRASP92: a package for large-scale relativistic atomic structure calculations. *Computer Phys Commun* 1996;94:249–71.
- [13] Sur C, Chaudhuri RK. Relativistic coupled-cluster calculation of core ionization potential using the normal and the semi-normal ordered ansatz. *J Phys B* 2004;37:4127–34;  
Sur C, Chaudhuri RK. A relativistic unitary coupled-cluster study of electric quadrupole moment and magnetic dipole hyperfine constants of  $^{199}\text{Hg}^+$ . *Phys Rev A* 2007;76:032503-1–7.
- [14] Pal'chikov VG. Relativistic transition probabilities and oscillator strengths in hydrogen-like atoms. *Phys Scr* 1998;57:581–93.
- [15] Plante DR, Johnson WR, Sapirstein J. Relativistic calculations of transition amplitudes in the helium isoelectronic sequence. In: Bederson B, Walther H, editors. *Adv At Mol Phys*, vol. 35. San Diego: Academic Press; 1995. p. 255–329.
- [16] Safranova UI, Safranova MS. Relativistic many-body calculations of E1, E2, M1 and M2 transitions rates for the  $1s2l2l' - 1s^22l$  lines in Li-like ions. *Mol Phys* 2004;102:1331–44.